Carbon nitride deposited using energetic species: A review on XPS studies

C. Ronning,* H. Feldermann, R. Merk, and H. Hofsäss
Universität Konstanz, Fakultät für Physik, Postfach 5560, D-78457 Konstanz, Germany

P. Reinke
Universität Basel, Institut für Physik, Klingelbergstrasse 82, CH-4056 Basel, Switzerland

J.-U. Thiele
IBM Almaden Research Center, San Jose, California 95120-6099
(Received 20 October 1997; revised manuscript received 26 January 1998)

This paper reviews x-ray photoelectron spectroscopy studies on carbon nitride (CN) and reports on results obtained from CN thin films prepared by mass selected ion-beam deposition. The core-level spectra of samples deposited at room temperature show that nitrogen is incorporated into the amorphous network in two different bonding configurations; carbon has three main bonding configurations whose relative contributions vary as a function of the nitrogen content. For samples deposited at elevated temperatures an ordering of the amorphous CN network towards a crystalline graphitelike structure is observed. Furthermore, both deposition at elevated temperatures (350 °C) and post-deposition ion irradiation have a strong influence on the bonding configuration in the CN films. Based on these results and the results reported in the reviewed literature a picture of the microstructure of carbon nitride deposited using energetic species is developed. [S0163-1829(98)03028-8]

I. INTRODUCTION

The theoretical predictions made by Liu and Cohen[1,2] on the existence of the covalent β-C_3N_4 compound with mechanical properties similar to diamond have triggered numerous experimental efforts to synthesize this material. In most cases vapor-phase methods like chemical vapor deposition, plasma deposition, and a variety of ion-assisted physical vapor deposition techniques were used to grow thin carbon nitride (CN) films (Refs. 3 and 4 and references therein). Up to now, the highest nitrogen content achieved in CN films deposited by these methods has not exceeded 50 at. %, and thus is still considerably below 57 at. % corresponding to the β-C_3N_4 phase. Also, experiments to implant high doses of nitrogen into carbon have not succeeded in achieving such high nitrogen concentrations.[5–9]

However, in an early study Marton *et al.* claimed the existence of a two-phase system in their CN films, where nanosized β-C_3N_4 crystallites might be embedded in an amorphous or graphitic carbon-rich matrix.[10] This study was based on x-ray photoelectron spectroscopy (XPS) measurements on CN films deposited with three different techniques and stimulated commensurate experiments by other groups. Similar XPS results were obtained and thus the successful synthesis of β-C_3N_4 was concluded (see, e.g., Refs. 7 and 11–13). In some cases, electron diffraction studies were performed to reinforce these conclusions,[7,12,14–17] but each of these studies shows different diffraction patterns. Additionally, the calculated theoretical lattice parameters vary[1,18] and the presented electron diffraction patterns can be plausibly accounted for by carbon phases.[18–20] Therefore, this analytical method is not suited to conclusively identify nanosized β-C_3N_4 crystallites embedded in an amorphous or/and graphitic carbon-rich matrix. An unequivocal identification of β-C_3N_4 by diffraction methods would only be possible with uniform stoichiometry having larger crystallites. XPS also cannot provide unambiguous evidence for the existence of β-C_3N_4 in such films. The energy distribution of the emitted core-level electrons, observed by XPS, reveals only the chemical environment of the atoms in the film. Structural information can be obtained with XPS only under specific circumstances. A distinction between amorphous and crystalline phases usually requires line-shape analysis and well-known and characterized reference samples.

In this paper, we present XPS measurements on CN films prepared with mass selected ion-beam deposition (MSIBD). With this technique the deposition conditions are precisely and independently controllable.[21,22] Therefore, MSIBD is most suitable to grow CN films under well-defined conditions. With MSIBD, the well-known diamondlike phase tetrahedral bonded amorphous carbon (ta-C) can also be produced.[23] We chose for this study parameters based on the preparation of ta-C films, since this should promote the formation of a tetrahedral CN phase. The chemical environment of the nitrogen and carbon atoms in the resulting CN films is studied as a function of nitrogen concentration and at two different substrate temperatures. First, as a basis for the discussion of our results, recent XPS studies on CN films with respective interpretations are reviewed. Based on a comparison with our data, and after a critical discussion, a model for the microstructure of CN films deposited using energetic species is proposed.

II. REVIEW OF RECENT XPS STUDIES

A common observation in nearly all recent XPS studies on CN films is that two and three contributions to the N 1*s* and C 1*s* core-level lines have to be assumed, respectively.[5–8,10–13,25–29,31–34] The binding energies reported for the components of the N 1*s* core-level line are generally

located around binding energies of 398 and 400 eV, i.e., separated by 1.7–2.2 eV. However, considerable variation in the C 1*s* core-level binding energy is found.

Marton and co-workers[3,10] presented N 1*s* and C 1*s* core-level spectra that were fitted with three and four lines, respectively. In each spectrum one minor line was attributed to oxygen surface contamination resulting in N-O or C-O bonds. From a comparison of two other lines of each spectrum to binding energies in pyridine (C_2H_5N) and urotropine ($C_6H_{12}N_4$) it was concluded that in the studied CN films a two-phase system exists, one with a tetrahedral type of binding configuration and one with a sp^2 configuration. Phase 1 is ''carbon and nitrogen atoms in positions resembling β-C_3N_4'' and phase 2 is ''areas with excess carbon.'' The lines were assigned as follows: 398.3 eV (N 1*s*) and 287.7 eV (C 1*s*) to phase 1; 400.0 eV (N 1*s*) and 285.9 eV (C 1*s*) to phase 2. This assignment seems questionable with regard to the relative contributions of each peak to the overall core-level line. Taking into account the different stoichiometries of the claimed phases, Marton and co-workers assign the major component in the C 1*s* to the minor component in the N 1*s* core-level line and vice versa. However, the remaining line of the C 1*s* spectrum at 284.6 eV, the highest intensity line, was completely ignored in this analysis. It is unlikely that about 50% of the overall detected carbon should be adventitious and surface carbon atoms without nitrogen neighbors.

This model was adopted by several groups to explain their XPS results on CN films prepared by different techniques (see, e.g., Refs. 7, 11–13, 24, 29, and 30). However, some variation in positions and intensities of the respective lines is found.[10,3]

A second set of publications[6,35] traces back to a study of Fujimoto and Ogata.[36] Their CN films prepared by ion-beam assisted deposition at low temperatures ($<100\,^{\circ}$C) show a shift of the C 1*s* core-level spectrum from 284.5 eV up to 286.3 eV as a function of nitrogen concentration. At high nitrogen concentrations, three lines were observed in the C 1*s* spectra and were attributed to diamond, graphite (or i-carbon), and ''a new material.'' However, up to now it is difficult to distinguish between graphite, amorphous carbon (a-C) and diamond from a C 1*s* analysis, because (i) the positions of the single C 1*s* lines are reported to be very close to each other around 284.7 eV (see, e.g., Refs. 37–39), and (ii) charging effects during analysis, which are present in the case of diamond and sometimes in a-C films. However, a large difference between diamond and graphite can be observed in the XPS valence-band spectra.[37–39] Furthermore, in the N 1*s* spectra presented by Fujimoto and Ogata[36] only one single line was observed at 398.4 eV in contrast to most other publications (see above).

In other studies[9,26–28,34,40] the two lines in the N 1*s* core-level spectra at 400 and 398 eV are attributed to N=C (imine) and N≡C (nitrile), respectively. This conclusion is also supported by *ab initio* based tight-binding molecular-dynamics simulations.[41] However, a comparison to infrared and/or Raman spectra, where N≡C bonds are clearly observable around 2200 cm^{-1}, shows that N≡C bonds play only a minor role in the CN network.[27,33,42,43] Therefore, it seems rather unlikely that this bonding type contributes 50% or more to the N 1*s* spectra.

Another interpretation of the N 1*s* core-level spectra was introduced by Sjöström *et al.*[31] The two nitrogen configurations were expected to be either N located in the hexagonal C planes or in a more tetrahedral-like position. The main line in their C 1*s* spectra was attributed to adventitious carbon, after Marton and co-workers.[3,10] However, even with a N/C ratio of 0.2–0.35 (i.e., 16–26 % nitrogen concentration) most carbon atoms statistically should have at least one nitrogen neighbor in a three-dimensional network. Furthermore, the films they prepared at high temperatures (600 °C) were superhard and elastic.[32] The authors found evidence and a satisfying explanation for these features by a fullerenelike microstructure, where substitutional nitrogen in the graphitic planes bends these into a wavy structure.

Finally, some authors give a mixture of the above-described interpretations to explain the XPS core-level spectra obtained from their CN films.[8,25,33]

III. EXPERIMENT

Carbon nitride thin films were grown on heatable Si-(100) substrates (T_S) by alternating deposition of $^{12}C^+$ and $^{14}N^+$ ions. Ions were accelerated up to 30 keV, mass separated and finally decelerated down to very low energies ($E_{\rm ion}$) of 50–100 eV to minimize physical and chemical sputter effects during growth.[33,42,44] The pressure in the UHV deposition chamber was less than 10^{-7} Pa during deposition. Typical ion current densities were $30-50\ \mu A/cm^2$ resulting in a growth rate of about 1 nm/min. Since nothing else than singly charged C^+ and N^+ ions are involved in this subsurface bulk-growth process under UHV conditions, the films are free of contaminants like oxygen, adventitious carbon, or hydrogen. Prior to deposition, the substrates were sputter-cleaned *in situ* with 1 keV $^{40}Ar^+$ ions. A uniform lateral deposition was achieved using a beam sweep in front of the deceleration stage. The details of the deposition system are described elsewhere.[21,22]

The amount of deposited material is determined with an accuracy of about 0.5% from measurements of the total deposited ion charge. The ion charge measurement is also used to switch the separation magnet between masses ^{12}C and ^{14}N, so that a constant C^+/N^+ ion ratio is maintained during film growth. During each switching cycle typically 5×10^{14} ions/cm^2 were deposited, thus ensuring a homogeneous film composition.

Immediately after deposition the films were characterized *in situ* by Auger electron spectroscopy (AES) and reflection electron energy-loss spectroscopy (EELS). For the EELS measurements a Perkin-Elmer CMA system was used, where electrons are detected in reflection geometry with primary electron energies of about 2 keV. The mean free path of electrons in this energy range is about 3 nm,[45] thus exceeding the ion range.

For XPS studies the samples were transferred into a UHV system (Leybold spectrometer, EA 11/100). A Mg K_α source ($h\nu=1253.6$ eV) was used; binding energies are referred to the Fermi level of a clean Au test sample and were calibrated using the Au $4f_{7/2}$ core line for which a binding energy of 84.0 eV is assumed. Energy resolutions of about 1.0 eV were obtained.

TABLE I. Deposition parameters and nitrogen concentration obtained by AES and XPS for CN films prepared by mass selected ion-beam deposition.

	Deposition parameters			Nitrogen concentration	
Sample	E_{ion} (eV)	T_s	C:N ratio	AES (at. %)	XPS (at. %)
162	100	RT	100:0	0	0
150	100	RT	97:3		3(1)
43	100	RT	90:10		7.5(2)
271	50	RT	83:17	11(3)	8(5)
272	50	RT	75:25	15(3)	11(5)
251	50	RT	40:60	33(3)	25(5)
273	50	350 °C	40:60	27(3)	21(5)

IV. STOICHIOMETRY

In Table I we have summarized the deposition parameters as well as the nitrogen concentration measured by *in situ* AES and *ex situ* XPS. AES spectra show only carbon and nitrogen peaks, whereas in the XPS spectra oxygen is also present due to the transfer through air. However, these contaminations are negligible (<5 at. %). The results from AES and XPS are in acceptable agreement within the error bars. They are plotted in Fig. 1 together with previously published Rutherford backscattering[42] and neutron depth profiling[46] data as a function of the provided N^+ ion fraction during deposition. For N^+ ion fractions below about 10% nearly all N^+ ions are incorporated into the film. Both a significant loss of N and a saturation of the N content at about 30 at. % take place if the N^+ ion fraction is increased up to about 70%. For N^+ ion fractions above 70% no film growth is observed, except the formation of thin silicon nitride surface layers. These effects are well known and can be explained by physical and chemical sputtering effects.[4,33,42,44]

V. ELECTRON ENERGY-LOSS SPECTROSCOPY

EELS measurements were carried out to obtain the plasmon energies of selected samples. For pure carbon films, which under these preparation conditions are tetrahedrally bonded and amorphous (ta-C) with a mass density of about 3 g/cm^3,[23] we measured plasmon energies of 32.0(3) eV. With increasing nitrogen concentration the plasmon energy decreases to 29.9(3) eV for sample 251. This means a lower electron density in the CN films and since nitrogen has five valence electrons in comparison to four valence electrons of carbon, it also indicates a strong decrease in the mass density of the CN films. This in good agreement with our previous results[42] and Refs. 28, 41, and 47.

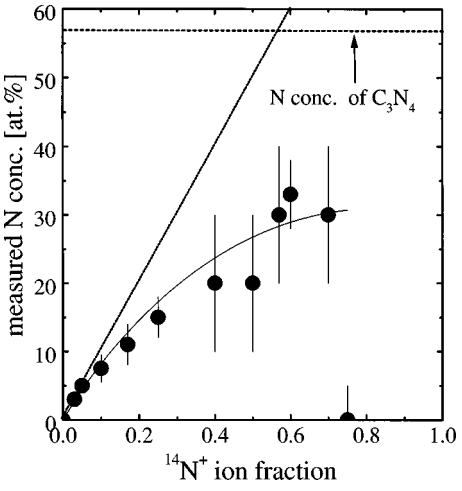

FIG. 1. Measured N concentration of CN films deposited onto Si at room temperature using $^{12}C^+$ and $^{14}N^+$ ions as a function of the N^+ ion fraction. For a N^+ ion fraction above 0.7 no CN film growth takes place (including data from Refs. 42 and 46).

VI. X-RAY PHOTOELECTRON SPECTROSCOPY

For a detailed analysis the core-level lines obtained by x-ray photoelectron spectroscopy were numerically fitted to Doniach-Sunjic functions, i.e., a convolution of a Gaussian and a Lorentzian profile with an additional parameter allowing asymmetry of the line.[48] In metals this asymmetry is directly related to the density of states at the Fermi level. Consequently the asymmetry should be zero in semiconducting or insulating materials. While in some cases it can be convenient to describe a number of symmetric lines by one asymmetric envelope (see, e.g., Ref. 49), here we tried to distinguish between the individual contributions. The asymmetry parameter α, however, proved to be useful to check the plausibility of the results of the fitting procedure, as explained in more detail below. The secondary (inelastically scattered) electron background to the lines was determined within the fitting procedure, assuming a background proportional to the respective integral intensity. During the fitting procedure all parameters were left free adjustable; the plausibility of the results was checked along the following lines.

The resolution of the analyzer used here is approximately 1 eV. This resolution mainly determines the linewidth of the Gaussian component of the Doniach-Sunjic function. Therefore, the fitting should yield at least 1 eV for the Gaussian linewidth of all components of a peak. Additionally, amorphization leads in general to a broadening of the linewidth. In this experiment we observed linewidths between 1.0 and 1.4 eV.

Not much is known about the relevance of the linewidth of the Lorentzian component of a peak in materials like the ones discussed here; however, a particular component can be expected to exhibit similar linewidths in similar films.

As mentioned above, the asymmetry of the various components should be close to zero in the case of a semiconduct-

TABLE II. Fitting results from the analysis procedure of the measured core-level lines. Lines were fitted to Doniach-Sunjic functions (Ref. 48). Whereas good agreement between measured and fitted lines for the N 1*s* spectra could be achieved in most cases with two Lorentzian lines, up to five lines had to be assumed for the C 1*s* spectra. Fractions were determined form the integrated areas of the lines. We labeled the lines *A*, *B*, and *C* for N 1*s* and from *D* through *H* for C 1*s*. *D** indicates a line at the same position of *D*, but with a different meaning as explained in the text.

	N 1*s*			C 1*s*				
Sample	*A*	*B*	*C*	*D*,*D**	*E*	*F*	*G*	*H*
162				284.9 eV				
				100 %				
150	399.4 eV			284.7 eV	285.4 eV			
	100%			35 %	65 %			
43	399.9 eV	399.3 eV		284.8 eV	285.7 eV			
	80 %	20 %		20 %	80 %			
271	399.9 eV	398.9 eV		284.7 eV	285.8 eV	286.5 eV	288.3 eV	
	74%	26 %		25 %	53 %	15 %	5 %	
272	399.8 eV	398.4 eV		284.6 eV	285.7 eV	286.8 eV	288.2 eV	
	80 %	20 %		25 %	55 %	14 %	5 %	
251	400.2 eV	398.2 eV		284.5 eV	285.5 eV	286.5 eV		
	60 %	40 %		44 %	36 %	20 %		
273	400.8 eV	398.2 eV	399.1 eV	284.7 eV	285.6 eV	286.4 eV	287.8 eV	289.9 eV
(T=350 C)	68 %	26 %	6 %	31 %	30 %	19 %	10 %	10 %

ing or insulating material—if the fitting yields larger deviations of the asymmetry parameter from zero and the films at the same time do not show a density of states at the Fermi level, this might be seen as an indication for the necessity of an additional component.

It almost goes without saying that the positions of individual components should not vary much from film to film. The results obtained by numerically fitting the experimental data for a series of films according to these guidelines are summarized in Table II. We labeled the lines *A*, *B*, and *C* for N 1*s* and from *D* through *H* for C 1*s*. *D** indicates a line at the same position of *D*, but with a different meaning as explained below.

A. N 1*s* core-level spectra of room-temperature deposited films

In Fig. 2 the XPS N 1*s* core-level spectra of all CN films deposited at room temperature with increasing N concentration are shown. For the lowest nitrogen concentration of 3 at. % (Fig. 2, top) a good agreement between the measured and fitted lines could be achieved with one peak, whereas two contributions had to be assumed for the other samples. The N 1*s* binding energy of sample 150 is 399.3 eV. With increasing nitrogen concentration up to about 9.5 at. % (average of AES and XPS) this line *A* shifts slightly to higher binding energies of 399.9 eV (samples 43 and 271) and remains there for further increase of the nitrogen concentration. The second line *B* emerges at a nitrogen concentration of about 7.5 at. % (sample 43). The position of this line shifts constantly from 399.3 eV for the 7.5 at. % sample to 398.2 eV for the 30 at. % sample. At the same time, the intensity of this line increases with growing nitrogen concentration.

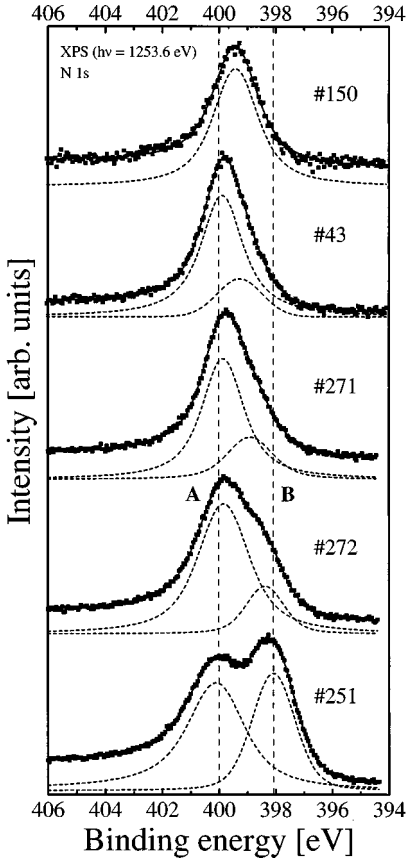

FIG. 2. XPS ($h\nu$=1253.6 eV) N 1*s* core-level spectra of CN samples prepared by MSIBD at room temperature as a function of nitrogen concentration (top, lowest concentration; bottom, highest concentration). Dots are the measured data and solid lines represent fits as described in the text. The dashed lines represent the two components obtained from the fit procedure.

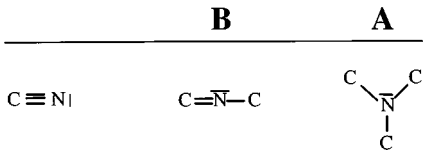

FIG. 3. Possible configurations of nitrogen atoms incorporated into an amorphous carbon network with one, two, or three neighbors.

Pure carbon films (ta-C) deposited at ion energies around 100 eV and at room temperature have a high mass density and consist of a highly tetrahedrally bonded amorphous network[23,50] (i.e., about 80–90% of the carbon atoms have four carbon neighbors). A nitrogen atom could be incorporated into an amorphous carbon network having a variety of different bonding environments with up to three neighbors as shown in Fig. 3. Based on theoretical studies[51–53] and the fact that a nitrogen atom cannot form five bonds, we can exclude configurations other than those shown in Fig. 3.

Moreover, one single neighbor can be excluded in our samples, since the triple bond plays only a minor role in the CN network as discussed above. With the incorporation of low concentrations (<10 at. %) of nitrogen no significant change of the dense amorphous network should occur, as observed by EELS. As a result of the above considerations, we assume that the N 1*s* line *A* around 400 eV originates from nitrogen atoms having three neighbors (Fig. 3). In this case, the films are best described as ''nitrogen-doped ta-C films,'' because the carbon atoms are still tetrahedrally coordinated. However, these films are not usable for electronic devices since only additional midgap and band-tail states are created.[46,53,54] The second line (*B*) in the N 1*s* spectra at around 398 eV is attributable to electrons originating from nitrogen atoms having two neighbors. Nitrogen atoms bound to their carbon neighbors in this way can also be a part of an aromatic ring system (e.g., like in pyridin). In samples with higher nitrogen concentration some neighbor atoms could be nitrogen instead of carbon. The difference in the N 1*s* binding energies would consequently be caused by the different hybridization: 3σ as opposed to $2\sigma+1\pi$, respectively. In agreement with Ref. 41, the decrease in the density of the CN films can then be explained with the lower coordination number of the nitrogen atoms.

This interpretation of our N 1*s* core-level spectra is supported by Boutique *et al.*[55] The measured N 1*s* core-level spectrum of 3,5,11,13-tetraazacycl(3.3.3)azine in this study shows two peaks separated by 3.0 eV with an intensity ratio of 1:4. The intense component at lower binding energy was attributed to the four nitrogen atoms in the molecule with two carbon neighbors and the line at higher binding energy to one nitrogen atom with three neighbors. Additionally, our interpretation is in agreement with Refs. 47 and 56 and close to that given by Sjöström *et al.*[31] In their interpretation the tetrahedral bonding is assumed to be achievable only in the configuration with bonds to four neighbor atoms. However, they did not consider the free orbital. A nitrogen atom σ-bonded to three carbon atoms and having one free orbital is tetrahedrally coordinated, e.g., NH_3. In accordance to the interpretation of Sjöström *et al.*, we assign the respective configuration to the lines observed in our N 1*s* spectra. A reverse assignment is quite possible, but fails if the respective stoichiometric amounts of the measured samples are considered (compare Tables I and II).

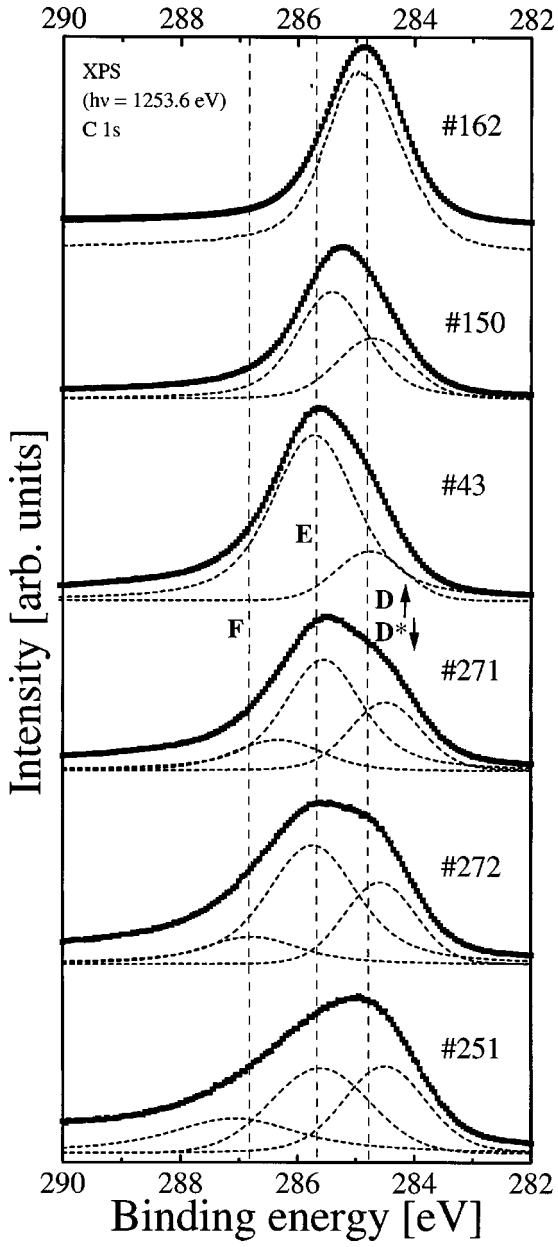

FIG. 4. XPS ($h\nu=1253.6$ eV) N 1*s* core-level spectra of CN samples prepared by MSIBD at room temperature as a function of nitrogen concentration (top, pure carbon; bottom, highest nitrogen concentration). Dots are the measured data and solid lines represent fits as described in the text. The dashed lines represent the three components obtained from the fit procedure.

Our interpretation of the N 1*s* core-level spectra is in contrast to Refs. 3, 10, 26–28, and 40, but we have a small amount of N≡C in our films, since we observe a small peak at 2200 cm^{-1} in the IR spectra.[42] According to Ref. 57, N≡C should form a line in the N 1*s* spectra at much higher binding energies compared to a nitrogen atom σ-bonded to three neighbors. We did not observe a line at such positions. This discrepancy might be due to a different IR sensitivity of the triple bond in relation to other bond configurations in CN films. Unfortunately, no investigations about the IR/Raman sensitivity factors were published to our knowledge.

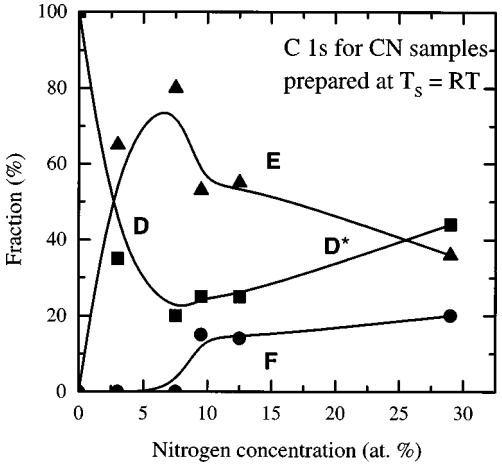

FIG. 5. Fraction of the components *D*, *D**, *E*, and *F* (from Table II) to the C 1*s* core-level spectra of CN films deposited at room temperature by MSIBD as a function of nitrogen concentration.

B. C 1*s* core-level spectra of room-temperature deposited films

Low nitrogen concentrations

For ta-C films a satisfactory agreement between the measured and fitted C 1*s* core-level spectrum could be achieved with one line (Fig. 4, top). The determined binding energy of 284.9 eV agrees well with the values of other pure carbon systems like graphite and diamond.[37–39] The full width at half maximum of this line is 1.5 eV. In the case of the samples with low nitrogen concentration (150 and 43) three lines were required to fit the measured C 1*s* spectra, which makes an interpretation much more difficult in comparison to the N 1*s* spectra. However, the contribution of the *F* component centered at 286.5 eV is almost negligible for these nitrogen concentrations. Component *D* centered at 284.7 eV decreases and component *E* centered at 285.7 eV increases with growing nitrogen concentration up to a nitrogen concentration of 7.5 at. %, as it can be seen in Figs. 4 and 5.

Analogous to the pure ta-C films, component *D* is ascribed to carbon atoms in a pure carbon environment for the nitrogen-doped ta-C films. In accordance with Ref. 59, we consequently ascribe component *E* to carbon atoms surrounded by three carbon and one nitrogen atom. The higher binding energy is attributed to an electron charge transfer from C to N.[1,2] The intensity ratio of the two lines *D* and *E* agrees well with the stoichiometry of the respective samples.

High nitrogen concentrations

With a further increase of the nitrogen concentration, component *F* becomes a significant part of the C 1*s* spectra (see Fig. 5) and four lines had to be used in order to achieve good agreement between fit and experimental data (Table II). However, the contribution of the fourth component is almost negligible (<5%) and is therefore not included in Figs. 4 and 5. The intensity ratio of components *D* and *E* now show an opposite behavior to that at low nitrogen concentrations, i.e., whereas component *D* increases as a function of nitrogen concentration, component *E* decreases (Fig. 5). In addition, we observe a slight shift of component *D* to lower binding energies leading to spectra similar to those observed by Marton and co-workers.[3,10] We assign now this component as *D**, indicating a different bonding configuration with equal binding energy.

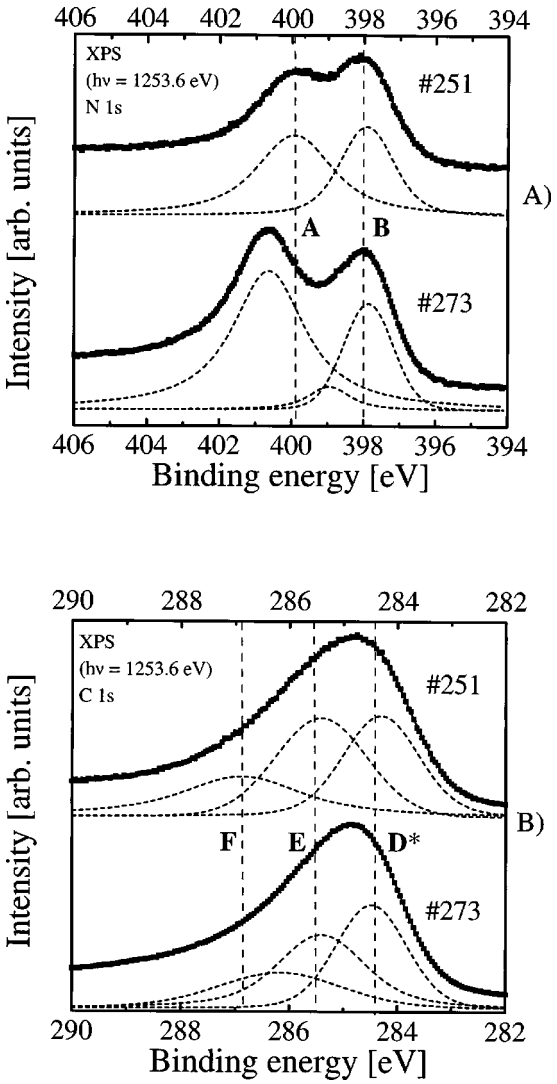

FIG. 6. N 1*s* (*A*) and C 1*s* (*B*) core-level spectra of CN films prepared by MSIBD with an ion ratio of C:N=4:6 at room temperature (top) and 350 °C (bottom).

Component *F* can be attributed to tetrahedrally bonded carbon atoms having two nitrogen neighbors due to a further increase of 1 eV in the binding energy. However, without doubt the films become more and more π-bonded with increasing nitrogen concentration as was concluded from EELS, density, and electrical measurements.[42] We assume that the additional π bond is much more effective at resisting charge transfer from C to N than a single σ bond. Such a change in the polarity of the π and σ C-N bond was already observed by Wan and Egerton.[58] Therefore, we claim that the origin of component *D** is due to sp^2 carbon bonded to carbon or nitrogen atoms. From this viewpoint, the intensities in the XPS spectra agree well with the stoichiometry of the CN films.

Summarizing the interpretation of the XPS core-level spectra, we would expect for the predicted β-C_3N_4 phase a single line at 400 eV in the N 1*s* spectra and a single line at

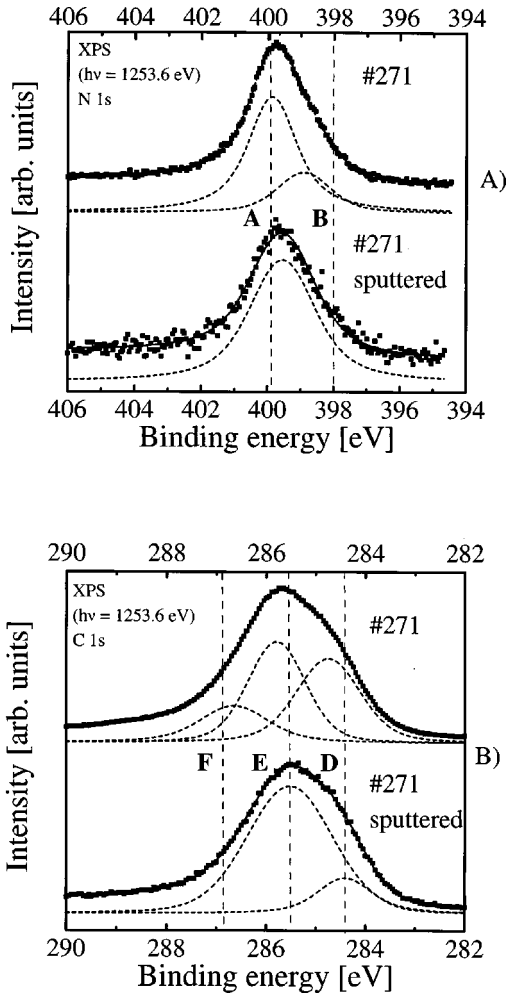

FIG. 7. N 1*s* (*A*) and C 1*s* (*B*) core-level spectra of sample 271 as deposited (top) and after 1 keV Ar-sputtering for 1 min (bottom).

high binding energies of about 288 eV in the C 1*s* spectra. This was not observed in any of the reviewed studies.

C. Influence of substrate temperature

Two samples with high nitrogen concentration were prepared by MSIBD at different substrate temperatures under otherwise unchanged conditions. Sample 251 was grown at room temperature and sample 273 at 350 °C (see Table I). The higher substrate temperature resulted in a considerably lower deposition rate due to the chemical sputtering effect at higher temperatures.[42,44] The XPS N 1*s* and C 1*s* core-level spectra of these two samples are shown in Figs. 6(a) and 6(b), respectively. While component *B* at low binding energies in the N 1*s* spectra was found to increase as a function of nitrogen concentration, component *A* at higher binding energies tends to increase as a function of deposition temperature. In addition, we observed a shift of this component towards higher binding energies. A third line (*C*) had to be fitted to the N 1*s* spectrum of sample 273, but the contribution of this line plays only a minor role [Fig. 6(a) (bottom)]. In the C 1*s* spectrum of the sample prepared at 350 °C, we measured only small differences in comparison to the room-temperature prepared sample [Fig. 6(b)]. We discovered a slight increase of line D^* at 284.5 eV at the expense of line *E* at 285.5 eV.

In light of our interpretation, we claim that for increasing deposition temperature an ordering of the amorphous CN network towards a graphitelike structure takes place, as observed by Sjöström *et al.*[31] This is supported by a separation and narrowing of the lines in the N 1*s* spectrum. In a graphitelike structure the N atoms are incorporated into the graphite planes having three neighbors forming pentagons, which results in the discovered wavy structure. The carbon atoms become increasingly sp^2 bonded with rising substrate temperature, which explains the increase of component D^* in the C 1*s* core-level spectrum.

D. Influence of sputtering

Sample 271, with a nitrogen content of 8 at. % (XPS data), was sputtered *in situ* with 1 keV Ar ions for 1 min after the above described measurements. Directly afterwards, XPS measurements were performed.

First, we observe a strong reduction of the nitrogen content to 5 at. %, in agreement with Ref. 13. However, this was expected due to the well-known preferential sputtering of nitrogen in CN films.[4,33,42,44] In Fig. 7 we have summarized the N 1*s* and C 1*s* core-level spectra obtained from the measurements before and after sputtering. The N 1*s* spectrum of the sputtered film requires only one line to achieve a good agreement between measured and fitted lines. The second component *B* at about 399 eV disappeared.

In the C 1*s* core-level spectra we observe a decrease of components *D* and *F* and a strong increase of component *E* [Fig. 7(b)]. Since the statistics in this spectrum are good enough, it seems that the tetrahedral configuration of carbon atoms containing one N neighbor is the most stable at these nitrogen concentrations, whereas sp^2 carbon is preferentially sputtered. Additionally, the signal of the tetrahedral carbon atoms with two N neighbors disappears due to nitrogen loss.

In summary, the XPS spectra of the sample after sputtering resemble those of an as deposited sample with the same nitrogen concentration (e.g., sample 43). From this experiment we can conclude that, apart from the preferential sputtering of nitrogen, sputtering has a strong influence on the bonding configuration in the CN films. This influence was also observed in diamond and amorphous carbon films.[60] Therefore, XPS measurements do not reflect the initial bond structure of CN films if the surface was cleaned by sputtering, as was the case in Refs. 7, 25, 27, 28, 33, and 36.

VII. CONCLUSIONS

CN thin films were grown by mass-separated ion beam deposition as a function of nitrogen concentration and at two substrate temperatures. The highest N content, corresponding to a C_2N stoichiometry, was achieved with an ion ratio of N:C=6:4. The N concentration is strongly limited due to chemical sputter processes during growth.

Room-temperature (RT) deposited CN films experience a reduction in the electron and mass density for increasing nitrogen concentrations. The core-level spectra show that nitrogen is incorporated into the amorphous network in two different bonding configurations. Carbon exists in three main bonding configurations as a function of the nitrogen concentration. We assume that the N 1*s* line *A* around 400 eV is due

to *s* electrons originating from nitrogen atoms having three neighbors, and the second line (*B*) in the N 1*s* spectra we attribute to *s* electrons originating from nitrogen atoms having two neighbors. The components *D* and *D** (around 284.7 eV), *E* (around 285.6 eV), and *F* (around 286.8 eV) in the C 1*s* core-level spectra were assigned as follows: *(D)* sp^3 carbon in a carbon environment for low nitrogen concentrations, (*D**) sp^2-bonded carbon for higher nitrogen concentrations, (*E*) sp^3-bonded carbon with one N neighbor, and *(F)* sp^3-bonded carbon with two N neighbors. This interpretation fits well with the respective measured stoichiometries and EELS results. At an elevated deposition temperature ordering of the amorphous CN network towards a crystalline graphitelike structure is observed.

ACKNOWLEDGMENTS

We would like to thank A. D. Banks for reading the manuscript. Financial support by the Deutsche Forschungsgemeinschaft under Grant No. HO1125/4-1 and Grant No. HO1125/8-1 under the auspices of the trinational D-A-CH cooperation on the ''Synthesis of Superhard Materials'' is gratefully acknowledged. J.-U. T. is grateful for funding by the Alexander-von-Humboldt-Stiftung (Bonn/Germany).

*Present address: Department of Materials Science and Engineering, North Carolina State University, Box 7919, Raleigh, NC 27695-7919.

Electronic address: Carsten_Ronning@ncsu.edu

[1] A. Y. Liu and M. L. Cohen, Science **245**, 841 (1994).

[2] A. Y. Liu and M. L. Cohen, Phys. Rev. B **41**, 10 727 (1990).

[3] D. Marton, K. J. Boyd, and J. W. Rabalais, Int. J. Mod. Phys. B **9**, 3527 (1995).

[4] B. Enders, Y. Horino, N. Tsubouchi, A. Chayahara, A. Kinomura, and K. Fujii, Nucl. Instrum. Methods Phys. Res. B **121**, 73 (1997).

[5] S. Grigull, W. Jacob, D. Henke, A. Mücklich, C. Spaeth, and L. Sümmchen, Appl. Phys. Lett. **70**, 1387 (1997).

[6] H. Xin, C. Lin, W. Xu, L. Wang, S. Zou, X. Wu, X. Shi, and H. Zhu, J. Appl. Phys. **79**, 2364 (1996).

[7] X. W. Su, H. W. Song, Q. Y. Zhang, and F. Z. Cui, Nucl. Instrum. Methods Phys. Res. B **111**, 59 (1996); J. Phys.: Condens. Matter **7**, L517 (1995).

[8] I. Gouzman, R. Brener, and A. Hofman, Thin Solid Films **253**, 90 (1994).

[9] L. Galan, I. Montero, and F. Rueda, Surf. Coat. Technol. **83**, 103 (1996).

[10] D. Marton, K. J. Boyd, A. H. Al-Bayati, S. S. Todorov, and J. W. Rabalais, Phys. Rev. Lett. **73**, 118 (1994).

[11] R. Zhong-Min, D. Yuan-Cheng, Y. Zhi-Feng, L. Fu-Ming, L. Jing, R. Yun-Zhu, and Z. Xiang-Fu, Nucl. Instrum. Methods Phys. Res. B **117**, 249 (1996).

[12] A. K. Sharma, P. Ayyub, M. S. Multani, K. P. Adhi, S. B. Ogale, M. Sunderaraman, D. D. Upadhyay, and S. Banerjee, Appl. Phys. Lett. **69**, 3489 (1996).

[13] S. Kumar, K. S. A. Butcher, and T. L. Tansley, J. Vac. Sci. Technol. A **14**, 2687 (1996).

[14] K. M. Yu, M. L. Cohen, E. E. Haller, W. L. Hansen, A. Y. Liu, and I. C. Wu, Phys. Rev. B **49**, 5034 (1994).

[15] C. Niu, Y. Z. Lu, and C. M. Lieber, Science **261**, 334 (1993).

[16] T.-Y. Yen and C.-P. Chou, Appl. Phys. Lett. **67**, 2801 (1995).

[17] L. A. Bursill, P. JuLin, V. N. Gurarie, A. V. Orlov, and S. Prawer, J. Mater. Res. **10**, 2277 (1995).

[18] D. M. Teter and R. J. Hemley, Science **271**, 53 (1996).

[19] J. V. Badding and D. C. Nesting, Chem. Mater. (to be published).

[20] N. V. Trubkin and M. I. Novgorodova, Crystallogr. Rep. **41**, 982 (1996).

[21] H. Hofsäss, H. Binder, T. Klumpp, and E. Recknagel, Diamond Relat. Mater. **3**, 137 (1994).

[22] H. Hofsäss and C. Ronning, in *Proceedings of the 2nd International Conference on Beam Processing of Advanced Materials*, edited by J. Singh, S. M. Copley, and J. Mazumder (ASM International, Materials Park, 1996), pp. 29–56.

[23] C. Ronning, E. Dreher, J.-U. Thiele, P. Oelhafen, and H. Hofsäss, Diamond Relat. Mater. **6**, 830 (1997).

[24] M. Tabbal, P. Merel, S. Moisa, M. Chaker, A. Ricard, and M. Moisan, Appl. Phys. Lett. **69**, 1698 (1996).

[25] J. H. Kim, D. H. Ahn, Y. H. Kim, and H. K. Baik, J. Appl. Phys. **82**, 658 (1997); Thin Solid Films **289**, 79 (1996).

[26] B. C. Holloway, D. K. Shuh, M. A. Kelly, W. Tong, J. A. Carlisle, I. Jimenez, D. G. I. Sutherland, L. J. Terminello, P. Pianetta, and S. Hagstrom, Thin Solid Films **290–291**, 94 (1996).

[27] S. Kobayashi, S. Nozaki, H. Morisaki, S. Fukui, and S. Masaki, Thin Solid Films **281–282**, 289 (1996).

[28] F. Rossi, B. Andre, A. van Veen, P. E. Mijnarends, H. Schut, F. Labohm, H. Dunlop, M. P. Delplancke, and K. Hubbard, J. Mater. Res. **9**, 2440 (1994); Thin Solid Films **253**, 85 (1994).

[29] A. Bousetta, M. Lu, and A. Bensaoula, J. Vac. Sci. Technol. A **13**, 1639 (1995).

[30] L. J. Huang, Y. Hung, S. Chang, G. R. Massoumi, W. N. Lennard, and I. V. Mitchell, J. Vac. Sci. Technol. A **15**, 2196 (1997).

[31] H. Sjöström, L. Hultman, J. E. Sundgren, S. V. Hainsworth, T. F. Page, and G. S. A. M. Theunissen, J. Vac. Sci. Technol. A **14**, 56 (1996).

[32] H. Sjöström, S. Stafström, M. Boman, and J. E. Sundgren, Phys. Rev. Lett. **75**, 1336 (1995).

[33] P. Hammer, M. A. Baker, C. Lenardi, and W. Gissler, Thin Solid Films **290–291**, 107 (1996); J. Vac. Sci. Technol. A **15**, 107 (1997).

[34] M. Ricci, M. Trinquecoste, F. Auguste, R. Canet, P. Delhaes, C. Guimon, G. Pflister-Guillouzo, B. Nysten, and J. P. Issi, J. Mater. Res. **8**, 480 (1993).

[35] Z. Ren, Y. Du, Y. Qiu, J. Wu, Z. Yiang, X. Xiong, and F. Li, Phys. Rev. B **51**, 5274 (1995); J. Phys. D **30**, 1370 (1997).

[36] F. Fujimoto, and K. Ogata, Jpn. J. Appl. Phys., Part 2 **32**, L420 (1993).

[37] F. R. McFeely, S. P. Kowalczyk, L. Ley, R. G. Cavell, R. A. Pollak, and D. A. Shirley, Phys. Rev. B **9**, 5268 (1974).

[38] R. G. Cedvall, S. P. Kowalczyk, L. Ley, R. A. Pollak, B. Mills, D. A. Shirley, and W. Perry, Phys. Rev. B **7**, 5313 (1973).

[39] H. Tsai and D. B. Body, J. Vac. Sci. Technol. A **5**, 3287 (1987).

[40] P. V. Kela, D. C. Cameron, B. J. Meenan, K. A. Pischow, and C. A. Anderson, N. M. D. Brown, and M. S. J. Hashmi, Surf. Coat. Technol. **74–75**, 696 (1995).

[41] F. Weich, J. Widany, and T. Frauenheim, Phys. Rev. Lett. **78**, 3326 (1997).

[42] H. Hofsäss, C. Ronning, U. Griesmeier, and M. Gross, in *Beam-Solid Interactions for Materials Synthesis and Characterization*,

edited by D. R. Luzzi *et al.*, MRS Symposium Proceedings No. 354 (Materials Research Society, Pittsburgh, 1995), p. 93.
[43] H. Xin, C. Lin, S. Zhu, S. Zou, X. Shi, H. Zhu, and P. L. F. Hemment, Nucl. Instrum. Methods Phys. Res. B **103**, 309 (1995).
[44] H. Hofsäss, C. Ronning, H. Feldermann, and M. Sebastian, in *Materials Modification and Synthesis by Ion Beam Processing*, edited by D. E. Alexander *et al.*, MRS Symposia Proceedings No. 438 (Materials Research Society, Pittsburgh, 1997), p. 575.
[45] H. Tokutaka, K. N. Nishimori, and H. Hayashi, Surf. Sci. **149**, 349 (1985).
[46] C. Ronning, U. Griesmeier, M. Gross, H. Hofsäss, R. G. Downing, and G. P. Lamaze, Diamond Relat. Mater. **4**, 666 (1995).
[47] C. Spaeth, M. Kuehn, F. Richter, U. Falke, M. Hietschold, R. Kilper, and U. Kreissig (unpublished).
[48] S. Doniach and M. Sunjic, J. Phys. C **3**, 285 (1970).
[49] J.-U. Thiele and P. Oelhafen, J. Nucl. Mater. **228**, 290 (1996).
[50] S. Christiansen, M. Albrecht, H. P. Strunk, C. Ronning, H. Hofsäss, and E. Recknagel, Diamond Relat. Mater. **7**, 15 (1998).
[51] P. Stumm and D. A. Drabold, Solid State Commun. **93**, 617 (1995).
[52] P. Stumm, D. A. Drabold, and P. A. Fedders, J. Appl. Phys. **81**, 1289 (1997).
[53] P. K. Sitch, T. Köhler, G. Jungnickel, D. Porezag, and T. Frauenheim, Solid State Commun. **100**, 549 (1996).
[54] H. Hofsäss, in Proceedings of the 1st International Specialist Meeting on Amorphous Carbon (World Scientific, Singapore, in press).
[55] J. P. Boutique, J. J. Verbist, J. G. Fripiat, J. Delhalle, G. Pfister-Guillouzo, and G. J. Ashwell, J. Am. Chem. Soc. **106**, 4374 (1984).
[56] J. R. Pels, F. Kapteijn, J. A. Moulijn, Q. Zhu, and K. M. Thomas, Carbon **33**, 1641 (1995).
[57] S. Huefner, *Photoelectron Spectroscopy: Principles and Applications* (Springer-Verlag, Berlin, 1995), p. 122.
[58] L. Wan and R. F. Egerton, Thin Solid Films **279**, 24 (1996).
[59] A. Mansour and D. Ugolini, Phys. Rev. B **47**, 10 201 (1993).
[60] P. Reinke, G. Franz, P. Oelhafen, and J. Ullmann, Phys. Rev. B **54**, 7067 (1996).